

Fullerene-like Colloidal Nanocrystal of Nickel Hydroxychloride

Shi Hu and Xun Wang*

Department of Chemistry, Tsinghua University, Beijing 100084, P. R. China

Received April 28, 2010; E-mail: wangxun@mail.tsinghua.edu.cn

Abstract: In this work, we successfully fabricated near-monodisperse colloids of a new type of inorganic fullerene-like structure (IF) of nickel hydroxychloride as the first example of the application of colloidal synthetic routes to the synthesis of IFs. The formation mechanism and interesting magnetic properties are briefly discussed.

Fullerene, as a new stable allotrope of carbon, has fascinated scientists around the world ever since its discovery¹ because of its delicate structure and novel properties. Fortunately, this kind of novel structure is not limited to carbon, and the pioneering work of Tenne and co-workers² on the successful synthesis of inorganic fullerene-like structures (IFs) of WS₂ opened more possibilities for the development of closed structures, including MoS₂,³ NiCl₂,⁴ CdI₂,⁵ NiBr₂,⁶ Ti₂O,⁷ GaSe,⁸ ReS₂,⁹ uranyl peroxide,¹⁰ and the like. However, successful examples of IF nanoparticles (NPs) are rare within the large store of layered inorganic substances because of the critical requirement of three-dimensional folding in space. Furthermore, the reported synthetic routes for IFs are usually based on extreme physical conditions that require high temperature, laser illumination, and/or high-vacuum systems, and the syntheses are usually haunted by low yield, poor dispersibility, and wide size distributions. Here we report the gram-scale synthesis of a new type of IFs of nickel hydroxychloride with a narrow size distribution and high yield via a facile solvothermal method.

There has been a great effort in the synthesis of monodisperse colloidal nanocrystals, including nanoparticles, nanorods, nanosheets, nanowires, etc., that can be used as the target of nanoscale materials research or as building blocks for macroscopic solids. Typical methods, ranging from hot-injection¹¹ and organic solvent-based methods¹² to solvothermal processes,¹³ initiate the reaction in a surfactant-confined microenvironment and render the processability and monodispersity. In this work, we successfully fabricated near-monodisperse colloidal IFs of nickel hydroxychloride as the first example of the application of colloidal synthetic routes to the synthesis of IF structures, which may establish a new methodology for the controllable fabrication of functional IFs.

The synthesis was based on a traditional colloidal synthetic route that has been well-studied. Typically, 2.2 mL of oleic acid (OA) was mixed with 0.6 mL of oleylamine (OM) in a 10 mL Teflon-lined autoclave and heated to 75 °C. Next, 1 mmol of NiCl₂·6H₂O was dissolved in 6 mL of ethanol through agitation or ultrasonication and added into the OA–OM mixture with stirring for 10 min, affording a transparent green solution. The autoclave was then sealed and heated at 200 °C for 4 h in an oven. After the system was cooled, the upper oil phase was decanted and the precipitate dispersed in cyclohexane. The dispersion was precipitated with ethanol to remove excess OA/OM and redispersed in cyclohexane. The final dispersion was transparent yellow-green and very stable for months (as shown in Figure 1a); meanwhile, an intense Tyndall effect was observed with an incident red laser (Figure 1a inset), showing the colloidal characteristics.

The morphology of the products was observed by transmission electron microscopy (TEM). The low-magnification TEM picture (Figure 1a) shows large areas of pure NPs with diameters of ~20 nm. These NPs took polyhedral shapes and were all hollow inside. High-resolution TEM (HRTEM, Figure 1d), showed that every NP was composed of nested multilayers with a lattice spacing of 0.56 nm while the center part was hollow or amorphous, which is the typical structure of IFs. It is worth noting that the NPs were not spherical (especially the smaller ones) and that layers usually had projections of polygons (most often pentagons) with large-angle turning points, as has been found in many other IF structures. The lattice contrast was lost around these turning points in the HRTEM pictures, similar to what was found in previous reports of WS₂ IFs; this might be caused by the breaking of atomic ordering. In a carbon-nanotube-based copper grid, amorphous materials were found joining adjacent IFs, which should be attributed to the OA/OM capping ligands, which endow them with good dispersibility in nonpolar solvents.

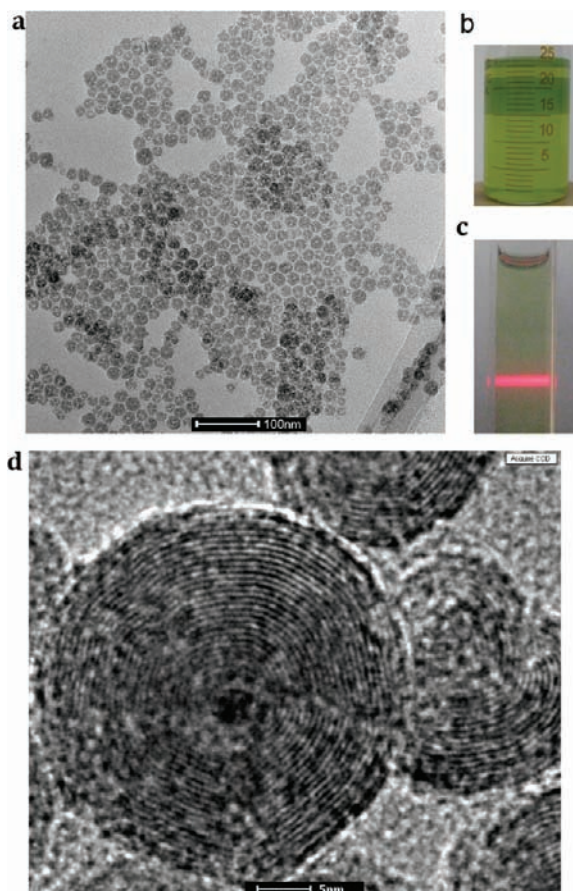


Figure 1. (a) TEM and (d) HRTEM pictures of IFs. (b) Cyclohexane dispersion of IF NPs and (c) the Tyndall effect it exhibited.

As for the chemical identity of this layered material, the X-ray diffraction (XRD) pattern (Figure S4 in the Supporting Information) showed a strong peak at $\sim 15.7^\circ$, whose position corresponds to the layer spacing measured using TEM, and peaks from 30 to 60° formed two big humps to which it was hard to index any deposited crystal profile. However, as similar layered structures have been found for NiCl_2 , $\text{Ni}(\text{OH})_2$, and $\text{Ni}_2\text{Cl}(\text{OH})_3$, we can give the empirical formula as $\text{NiCl}_{0.78}(\text{OH})_{1.22} \cdot x\text{H}_2\text{O}$ on the basis of elemental analysis. While the TGA curve (Figure S5) indicated a gradual slope before 300°C resulting from the loss of OA/OM, the peak at 1612 cm^{-1} in the FTIR spectrum (Figure S3) showed that the primary ligand was OM, as the signature peak for OA ($\sim 1700\text{ cm}^{-1}$) was almost unobservable. The strong absorption peak at 3581 cm^{-1} in the IR spectrum should be attributed to the abundance of OH^- in the inorganic framework of nickel hydroxychloride.

In this new colloidal system, it was of interest to probe the mechanism for the generation of IFs. Here the morphology evolution of final products with different reaction times at 185°C was carefully studied using TEM. As shown in Figure 2, at the very beginning of the reaction, a large amount of tiny crystallites with diameters of $\sim 3\text{ nm}$ was found. With increasing time, the nanocrystallites were consumed, while some faceted few-layer fullerene NPs with amorphous cores having diameters of less than 10 nm appeared. As these IFs grew,

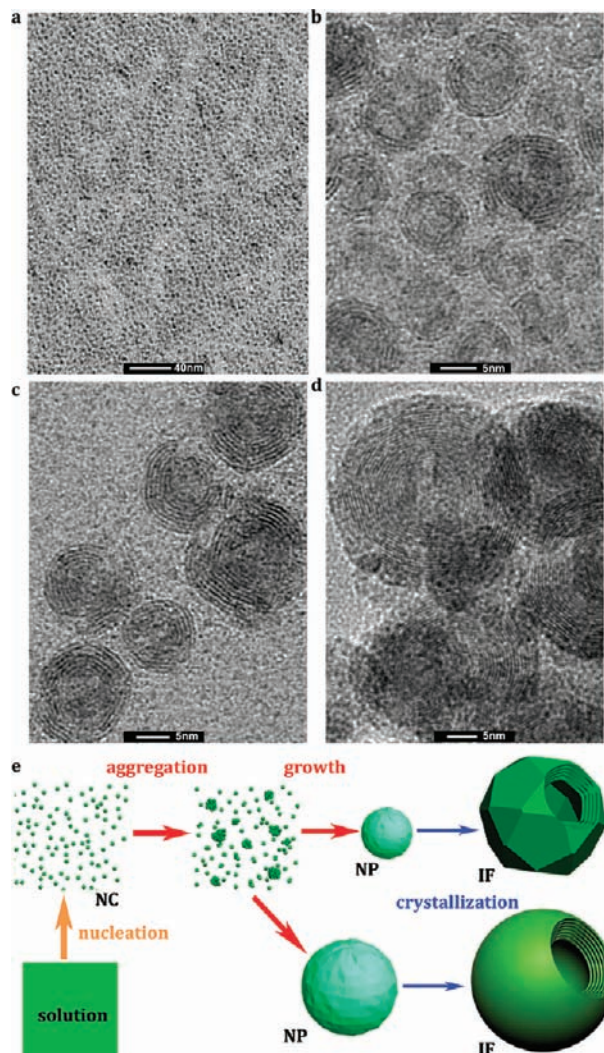


Figure 2. (a–d) Typical TEM pictures of products after reaction at 185°C for (a) 1, (b) 2, (c) 3, and (d) 8 h. (e) Schematic diagram showing the mechanism of NP aggregation and growth followed by IF formation.

the number of layers increased until finally IFs with diameters of $\sim 20\text{ nm}$ dominated. Hence, a three-step “nucleation–assembly–recrystallization” mechanism would be more reasonable under solvothermal conditions: tiny nanocrystallites nucleate from the solution at elevated temperature and gradually aggregate into bigger NPs with OA/OM molecules capping the surface; these NPs then develop layered fullerene-like structures from outside. Specifically, when the size of the NP is relatively large (i.e., 25 nm), circular bending of the layers is favored, while in smaller NPs, the tension of layer bending increases, allowing only faceted IFs with the presence of large-angle turning points in the layers.

The as-synthesized fullerene-like nickel hydroxychloride ($\text{Ni}-\text{Cl}-\text{OH}$) is among a family of triangular layered compounds that has aroused increasing interest in the study of exotic magnetic properties such as geometrically frustrated magnetism.¹⁴ It was found that some transition-metal compounds with the chemical formula of $\text{M}_2\text{X}(\text{OH})_3$ share a common feature of coexisting long-range order (ferromagnetic or antiferromagnetic) and spin fluctuations¹⁵ under the phase-transition point. Figure 3 shows the temperature dependence of the susceptibility of the IF sample under field cooling (FC) and zero-field cooling (ZFC) conditions; the two curves diverge at around 16 K from above, indicating a coexisting glassiness at low temperature that gives rise to the increase in susceptibility. Further experiments concerning the relationship of the magnetic behavior and the IF size are in progress.

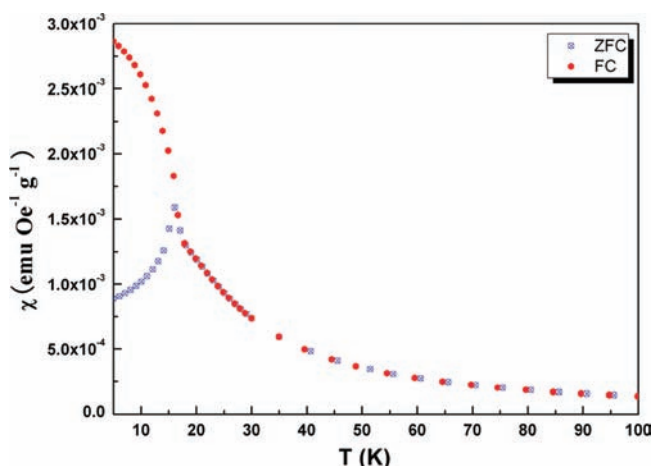


Figure 3. Magnetization curve under FC and ZFC conditions.

In summary, we have employed the well-established colloidal synthetic route for the large-scale fabrication of monodisperse inorganic fullerenes of nickel hydroxychloride. These IF nanoparticles can be well-dispersed in nonpolar organic solvents, thus paving the way for easy film or composite fabrication with novel functions. On the other hand, this material exhibits a magnetic phase transition at low temperature that provides a new platform for the study of exotic magnetic phenomena on the nanoscale.

Acknowledgment. This work was supported by NSFC (Grant 20725102) and the State Key Project of Fundamental Research for Nanoscience and Nanotechnology (Grant 2006CB932301).

Supporting Information Available: Additional TEM pictures, EDS data, FTIR spectrum, XRD pattern, and TGA and DTA curves for the IFs. This material is available free of charge via the Internet at <http://pubs.acs.org>.

References

- (1) Kroto, H. W.; Heath, J. R.; O'Brien, S. C.; Curl, R. F.; Smalley, R. E. *Nature* **1985**, *318*, 162.
- (2) Tenne, R.; Margulis, L.; Genut, M.; Hodes, G. *Nature* **1992**, *360*, 444.

- (3) Margulis, L.; Salitra, G.; Tenne, R.; Talianker, M. *Nature* **1993**, *365*, 113.
- (4) Hacothen, Y. R.; Grunbaum, E.; Tenne, R.; Sloan, J.; Hutchison, J. L. *Nature* **1998**, *395*, 336.
- (5) Popovitz-Biro, R.; Sallacan, N.; Tenne, R. *J. Mater. Chem.* **2003**, *13*, 1631.
- (6) Bar-Sadan, M.; Popovitz-Biro, R.; Prior, Y.; Tenne, R. *Mater. Res. Bull.* **2006**, *41*, 2137.
- (7) Avivi, S.; Mastai, Y.; Gedanken, A. *J. Am. Chem. Soc.* **2000**, *122*, 4331.
- (8) Gautam, U. K.; Vivekchand, S. R. C.; Govindaraj, A.; Kulkarni, G. U.; Selvi, N. R.; Rao, C. N. R. *J. Am. Chem. Soc.* **2005**, *127*, 3658.
- (9) Yella, A.; Therese, H. A.; Zink, N.; Panthofer, M.; Tremel, W. *Chem. Mater.* **2008**, *20*, 3587.
- (10) Forbes, T. Z.; McAlpin, J. G.; Murphy, R.; Burns, P. C. *Angew. Chem., Int. Ed.* **2008**, *47*, 2824.
- (11) Peng, X. G.; Wickham, J.; Alivisatos, A. P. *J. Am. Chem. Soc.* **1998**, *120*, 5343.
- (12) Sun, S. H.; Murray, C. B.; Weller, D.; Folks, L.; Moser, A. *Science* **2000**, *287*, 1989.
- (13) Wang, X.; Zhuang, J.; Peng, Q.; Li, Y. D. *Nature* **2005**, *437*, 121.
- (14) Lee, S. H.; Kikuchi, H.; Qiu, Y.; Lake, B.; Huang, Q.; Habicht, K.; Kiefer, K. *Nat. Mater.* **2007**, *6*, 853.
- (15) Zheng, X. G.; Nishiyama, K. *Physica B* **2006**, *374*, 156.

JA103607Q